



Analysis of the Impact of Disruptions from the Launch of Missile on the Stability of a Scanning and Tracking IR Seeker Operation

Daniel GAPIŃSKI

*Kielce University of Technology Faculty of Mechatronics and Mechanical Engineering,
7 1000-lecia Państwa Polskiego Avenue, 25-314 Kielce, Poland
Author's email address: tu_daniel_kielce@wp.pl*

Received by the editorial staff on 14 November 2016

Reviewed and verified version received on 26 January 2017

DOI 10.5604/01.3001.0010.1572

Abstract. The paper presents the results of research to determine the impact of disruptions occurring during the launch of missile on the stability of operation of an optoelectronic scanning and tracking IR seeker (homing head). The main task of the seeker is to detect and then precisely track an air target. In the tests, the dynamic disruptions due to overloads acting on the seeker during the launch of the missile system were taken into account. The test results are presented in a graphic form

Keywords: mechanics, homing IR seeker, overloads, missile, launch of phase

1. INTRODUCTION

Figure 1 presents a 3D visualization of the designed optoelectronic scanning and tracking IR seeker (homing head). [1] and the coordinate systems adopted for its analysis.

The primary intended use of the seeker is to detect and then precisely track an air target. The construction, principle of operation as well as dynamics analysis of the seeker are presented in other reports [2]. The methods used to control the device as well as the opportunity to track air targets that move at supersonic speeds are also presented in other reports [3, 4, 5].

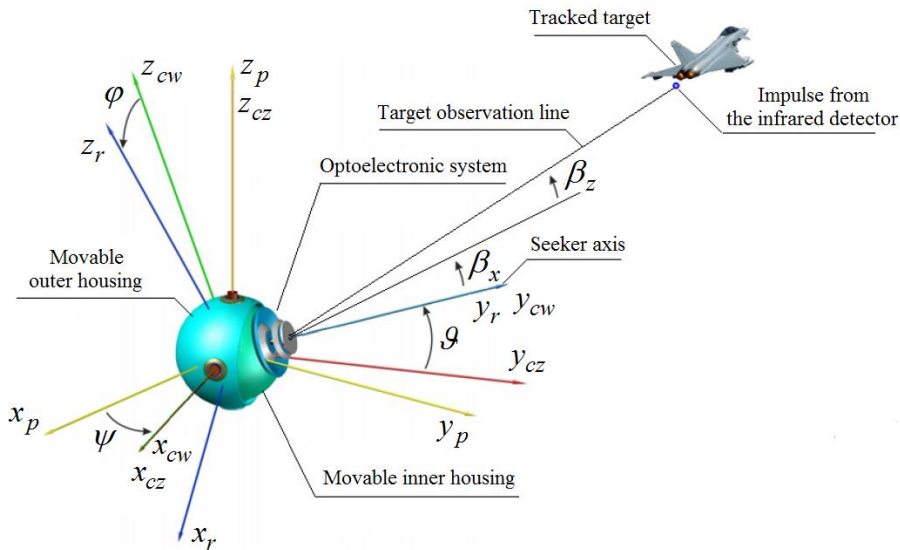


Fig. 1. IR seeker and the adopted coordinate systems

With the constantly improving manoeuvring abilities of air attack measures [6, 7], the requirements to be met by a homing, close-range missile also need to change. The most important of these include an increase in flight velocity and an improvement in manoeuvrability, which automatically changes the requirements concerning search-track seeker [8, 9]. Along with these changes in the missile parameters, the overloads to which the homing head is subject also increase. Prior to the launch of the missile, during the homing head's airspace search phase, a number of adverse conditions may occur as the result of the angular displacement of the launcher itself, which may be located on board a warship rolling at sea [10, 11]. This work presents an analysis of the impact of this type of disruption on the accuracy of determining the location of an air target by the proposed scan-track seeker [12]. While tracking an already detected air target, adverse dynamic inputs may occur during the launch of the missile.

The most significant impact on the formation of this type of input result from the longitudinal overloads of a missile as well as any simultaneous tilt of the missile once the missile launcher is lowered.

These disruptions may adversely affect the correct determination of the angular coordinates of a detected air target, marked in Fig. 1 as β_x and β_z . For this reason, it is important to determine the values of this type of overload as well as their impact on the stability of device operation.

2. MATHEMATICAL MODEL

Figure 2 shows the dynamic forces acting on the individual elements of the homing head, resulting from the extra loads that impact a missile during the initial phase of its flight. This phase covers the period from the moment of launch of the missile from the launcher to the moment the missile reaches its optimum cruising speed [13].

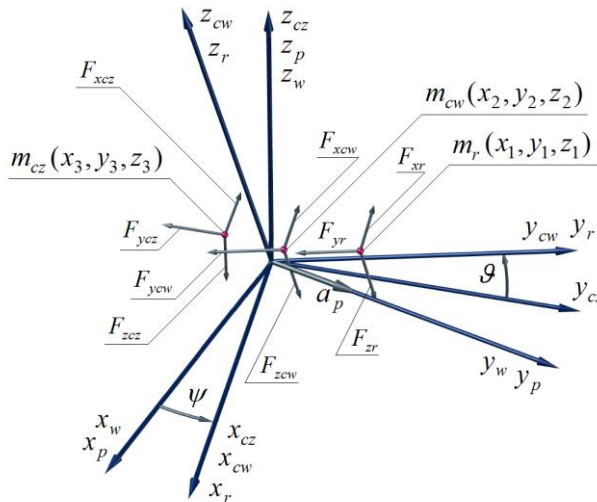


Fig. 2. Forces acting on the IR seeker – resulting from missile overloads

For the purposes of analysing the impacts of these disruptions occurring during the launch of the missile on the stability of operation of the designed scan-track seeker, the following coordinate systems were adopted:

- x_w, y_w, z_w – inertial coordinate system (reference frame),
- x_r, y_r, z_r – coordinate system connected with the seeker rotor,
- x_{cw}, y_{cw}, z_{cw} – coordinate system connected with the inner housing,
- x_{cz}, y_{cz}, z_{cz} – coordinate system connected with the outer housing,
- x_p, y_p, z_p – coordinate system connected with the missile.

Also, the following angles of rotation were adopted:

ψ – angle of rotation $x_{cz} y_{cz} z_{cz}$ in relation to $x_p y_p z_p$ around axis z_{cz} ,

\mathcal{G} – angle of rotation $x_{cw} y_{cw} z_{cw}$ in relation to $x_p y_p z_p$ around axis x_{cw} .

The seeker optical axis is set in set motion under the influence of moments of external forces M_z and M_w generated by the control motors located in the individual control housings. The values of the set control moments have to compensate for both disruptions due to the angular velocities of the missile deck ω_{xp} , ω_{yp} , ω_{zp} causing its rotation by the angles α_{xp} α_{yp} α_{zp} (in relation to the system $x_w y_w z_w$), and also compensation of the moments triggered by the forces of inertia due to the overloads acting on the missile during the launch of phase. The dynamic forces acting on the individual elements of the homing seeker are at equilibrium with the forces of inertia resulting from the overloads acting on the missile during launch of phase. It can be assumed with suitable accuracy that, during the launch of a missile, the largest component of the overload acts along its longitudinal axis, marked in Figs. 1 and 2 as y_p . The above component is marked in Fig. 2 as the complete acceleration of the missile a_p . If we consider the rotor total mass as m_r and concentrate it at the material particle with the same name described by the coordinates x_1, y_1, z_1 that determine the position of the centre of mass of the rotor in relation to the adopted coordinate system $x_r y_r z_r$, then the force of inertia of this particle is $\vec{F}_r = -\vec{a}_p \cdot m_r$. If we consider the seeker inner housing total mass as m_{cw} and concentrate it at the material particle with the same name described by the coordinates x_2, y_2, z_2 that determine the position of the centre of mass of the inner housing in relation to the adopted coordinate system $x_{cw} y_{cw} z_{cw}$, then the force of inertia of this particle will be $\vec{F}_{cw} = -\vec{a}_p \cdot m_{cw}$. Analogically, if we consider the seeker outer housing total mass as m_{cz} and concentrate it at the material particle with the same name described by the coordinates x_3, y_3, z_3 that determine the position of the centre of mass of the outer housing in relation to the adopted coordinate system $x_{cz} y_{cz} z_{cz}$, then the force of inertia of this particle will be $\vec{F}_{cz} = -\vec{a}_p \cdot m_{cz}$. However, each of the above forces can be resolved into three compounds parallel to the axes of the corresponding coordinate systems, as illustrated in Fig. 2. These compounds will have the following values, respectively:

$$F_{xr} = -m_r \cdot a_p \cdot \sin \psi \quad (1)$$

$$F_{yr} = -m_r \cdot a_p \cdot \cos \psi \cdot \cos \mathcal{G} \quad (2)$$

$$F_{zr} = -m_r \cdot a_p \cdot \sin \mathcal{G} \quad (3)$$

$$F_{xcw} = -m_{cw} \cdot a_p \cdot \sin \psi \quad (4)$$

$$F_{ycw} = -m_{cw} \cdot a_p \cdot \cos \psi \cdot \cos \mathcal{G} \quad (5)$$

$$F_{z_{cw}} = -m_{cw} \cdot a_p \cdot \sin \vartheta \quad (6)$$

$$F_{x_{cz}} = m_{cz} \cdot a_p \cdot \sin \psi \quad (7)$$

$$F_{y_{cz}} = -a_y \cdot m_{cz} \cdot \cos \psi \quad (8)$$

$$F_{z_{cz}} = 0 \quad (9)$$

The forces described by equations (1-9) cause the formation of moments of forces around the axis of rotation of the inner housing M_{PW} and of the outer housing M_{PZ} , as described by the following dependences:

$$M_{Wp} = F_{yr} \cdot |z_1| - F_{zr} \cdot |y_1| + F_{ycw} \cdot |z_2| - F_{z_{cw}} \cdot |y_2| \quad (10)$$

$$M_{Zp} = F_{y_{cz}} \cdot |x_3| + F_{x_{cz}} \cdot |y_3| + F_{x_{cw}} \cdot \cos \vartheta \cdot |y_2| - F_{y_{cw}} \cdot \cos \vartheta \cdot |x_2| + \quad (11)$$

$$+ F_{x_r} \cdot \cos \vartheta \cdot |y_1| - F_{y_r} \cdot \cos \vartheta \cdot |x_1|$$

Where the positions of the centres of mass of the individual elements of the rotor are, respectively:

- The position of the centre of mass of the rotor in relation to the axis x_r, y_r, z_r :
 $x_1 = 0 \text{ m}; y_1 = 0.0128 \text{ m}; z_1 = 0.000234 \text{ m}$
- The position of the centre of mass of the inner housing in relation to the axis x_{cw}, y_{cw}, z_{cw} :
 $x_2 = 0 \text{ m}; y_2 = 0.000642 \text{ m}; z_2 = 0.001854 \text{ m}$
- The position of the centre of mass of the outer housing in relation to the axis x_{cz}, y_{cz}, z_{cz} :
 $x_3 = 0.0063 \text{ m}; y_3 = -0.0122 \text{ m}; z_3 = -0.00192 \text{ m}$

On the basis of the adopted physical model, and by making use of second order Lagrange equations, the following equations for the motion of the seeker axis were derived:

$$J_{z_{cz}} \frac{d}{dt} \omega_{z_{cz}} + J_{y_{cw}} \frac{d}{dt} (\omega_{y_{cw}} \sin \vartheta) + J_{z_{cw}} \frac{d}{dt} (\omega_{z_{cw}} \cos \vartheta) +$$

$$+ J_{y_r} \frac{d}{dt} (\omega_{y_r} \sin \vartheta) + J_{z_r} \frac{d}{dt} (\omega_{z_r} \cos \vartheta) - (J_{x_{cz}} - J_{y_{cz}}) \omega_{x_{cz}} \omega_{y_{cz}} + \quad (12)$$

$$- (J_{x_{cw}} + J_{x_r}) \omega_{x_{cw}} \omega_{y_{cz}} + J_{y_{cw}} \omega_{y_{cw}} \omega_{x_{cz}} \cos \vartheta +$$

$$- (J_{CW} + J_{z_r}) \omega_{z_{cw}} \omega_{x_{cz}} \sin \vartheta + J_{y_r} \omega_{y_r} \omega_{x_{cz}} \cos \vartheta = M_Z - M_{TZ} - M_{Zp}$$

$$J_{x_{cw}} \frac{d}{dt} \omega_{x_{cw}} + J_{x_r} \frac{d}{dt} \omega_{x_{cw}} - (J_{y_{cw}} - J_{z_{cw}} - J_{z_r}) \omega_{y_{cw}} \omega_{z_{cw}} +$$

$$- J_{y_r} \omega_{y_r} \omega_{z_{cw}} = M_W - M_{TW} - M_{Wp} \quad (13)$$

with:

- $\omega_{xCZ} = \omega_{xp} \cos \psi + \omega_{yp} \sin \psi$
- $\omega_{yCZ} = -\omega_{xp} \sin \psi + \omega_{yp} \cos \psi$
- $\omega_{yCW} = \omega_{yCZ} \cos \vartheta + \omega_{xCZ} \sin \vartheta$
- $\omega_{zCW} = -\omega_{yCZ} \sin \vartheta + \omega_{zCZ} \cos \vartheta$
- $J_{xCZ}, J_{yCZ}, J_{zCZ}$ – moments of complete inertia of the outer housing,
- $J_{xCW}, J_{yCW}, J_{zCW}$ – moments of complete inertia of the inner housing,
- J_{xR}, J_{yR}, J_{zR} – moments of inertia of the rotor,
- $\vec{\omega}_p (\omega_{xp}, \omega_{yp}, \omega_{zp})$ – angular velocity of the missile,
- \vec{M}_z – moment controlling the seeker outer housing,
- \vec{M}_w – moment controlling the seeker inner housing,
- $\vec{M}_{TW}, \vec{M}_{TZ}$ – moments of friction forces in the bearings of, respectively, the inner and outer housings, and $\vec{M}_{TW} = c_w \dot{\vartheta}$, $\vec{M}_{TZ} = c_z \dot{\psi}$

where:

c_w – coefficient of friction in the inner housing bearing,

c_z – coefficient of friction in the outer housing bearing,

$\vec{M}_{wp}, \vec{M}_{zp}$ – moments of forces due to the acceleration of the missile in the initial phase of its flight, acting respectively on the seeker inner and outer housings.

Disturbing moments M_{wp}, M_{zp} may adversely affect the correct operation of the seeker, and for this reason it is important to determine their impact on the stability of device operation. The general analysis of the stability of operation of the seeker was carried out with the use of Lyapunov's direct method (presented in [14]), where the aforementioned stability analysis was extended to include interfering moments M_{wp} and M_{zp} in the mathematical model.

3. TEST RESULTS

The above paragraph presents selected examples of the computer simulations used for the dynamic loads acting on the basic elements of the presented scan-track seeker during the launch of a missile as well as interfering control moments of the outer and inner housings created as a result of the aforementioned loads.

3.1. Seeker Parameters

- Rotor mass: $m_r = 1.753$ kg
- Inner housing mass: $m_{cw} = 0.45$ kg
- Outer housing mass: $m_{cz} = 0.06$ kg
- Moments of inertia of the rotor in relation to the axis x_R, y_R, z_R :
 $J_{xR} = 0.00158446$ kgm²
 $J_{yR} = 0.0011405$ kgm²
 $J_{zR} = 0.00158124$ kgm²
- Moments of complete inertia of the inner housing in relation to the axis x_{cW}, y_{cW}, z_{cW} :
 $J_{x_{cW}} = 0.00044593$ kgm²
 $J_{y_{cW}} = 0.00064376$ kgm²
 $J_{z_{cW}} = 0.00047213$ kgm²
- Moments of complete inertia of the outer housing in relation to the axis x_{cZ}, y_{cZ}, z_{cZ} :
 $J_{x_{cZ}} = 0.00020254$ kgm²
 $J_{y_{cZ}} = 0.00032367$ kgm²
 $J_{z_{cZ}} = 0.00022394$ kgm²
- Coefficient of friction in the inner housing bearing:
 $c_w = 0.05$ Nms
- Coefficient of friction in the outer housing bearing:
 $c_z = 0.05$ Nms

3.2. Analysis of disruptions due to the launch of the missile

Figure 3 presents the velocity of the missile in the initial phase of its flight, while Fig. 4 presents the acceleration acting on the missile in the course of its flight, used to calculate the dynamic forces acting on the seeker. In addition, the simulations take into account the seeker static imbalance resulting directly from its construction and inaccuracy of execution. The longitudinal overload occurring during the launch of the missile will exercise the most adverse impact on the seeker operation in those cases where its optical axis does not overlap the missile axis. This type of situation is also taken into account in the simulations. Figs. 7, 8, 11 and 12 present the resultant dynamic interfering moments, acting respectively on the homing seeker outer and inner housings during the launch of the missile.

The simulations also took into account the fact that the seeker optical axis does not overlap the missile axis, by setting the seeker axis in a motion that was selected by rotating the outer housing, as illustrated in Figs. 5 and 9, as well as by rotating the inner housing, as illustrated in Figs. 6 and 10.

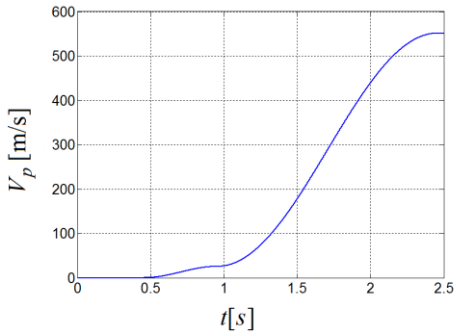


Fig. 3. Missile velocity

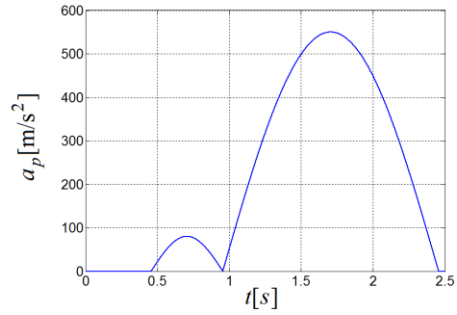


Fig. 4. Longitudinal overloads of the missile

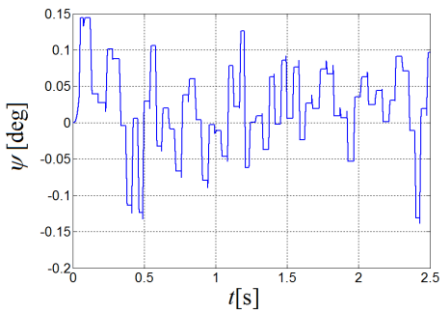


Fig. 5. Angle of rotation of the outer housing

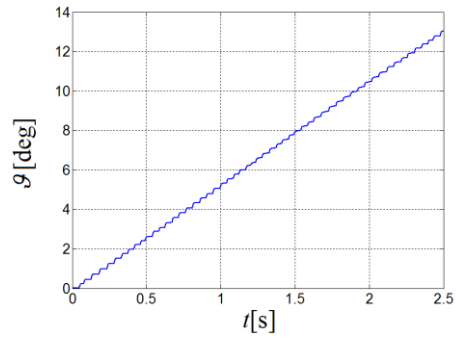


Fig. 6. Angle of rotation of the inner housing

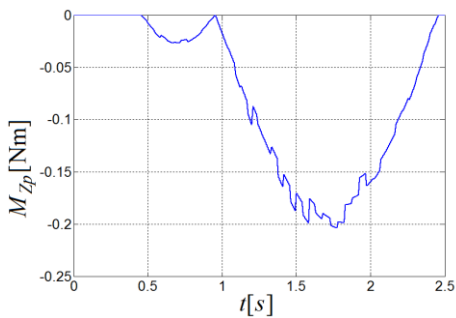


Fig. 7. Moment of force interference acting on the outer housing

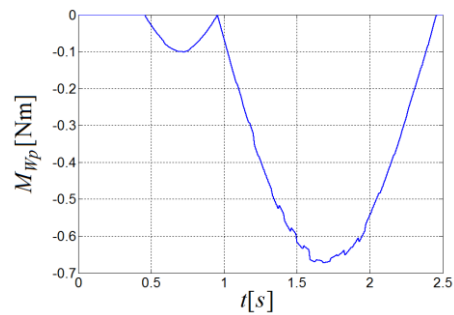


Fig. 8. Moment of force interference acting on the inner housing

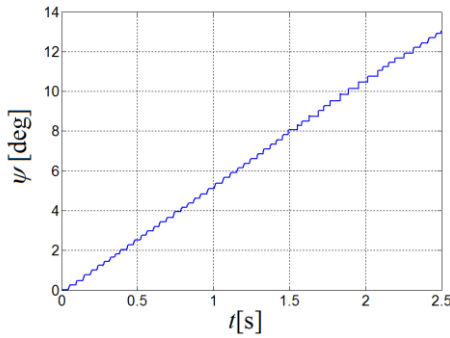


Fig. 9. Angle of rotation of the outer housing

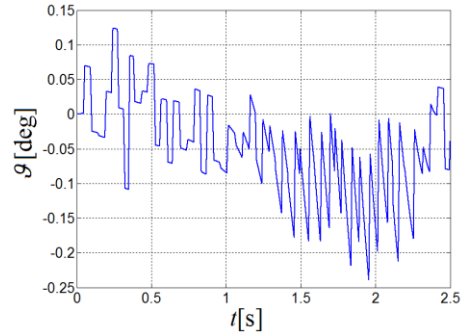


Fig. 10. Angle of rotation of the inner housing

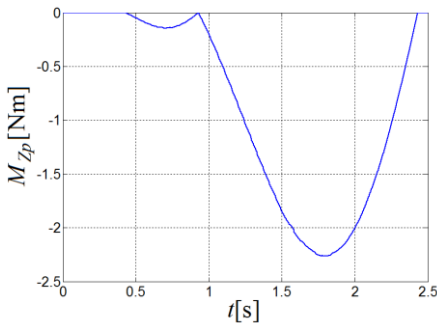


Fig. 11. Moment of force interfering acting on the outer housing

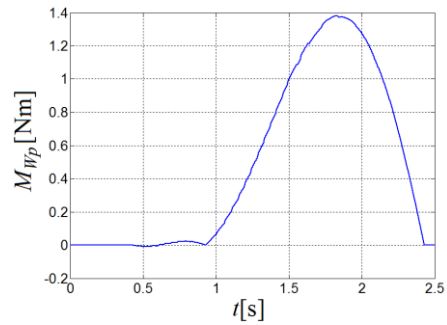


Fig. 12. Moment of force interfering acting on the inner housing

3.3. Analysis of disruptions during the launch of the missile with the seeker static balance taken into account

The seeker static balance should result in the accurate overlapping of the centre of mass of the rotor m_r , the centre of mass of the outer housing m_{cz} and the centre of mass of the inner housing m_{cw} with the point of intersection of the axis of rotation of the outer and inner housings.

It is impossible to obtain perfect static balance under real conditions, but it may effectively limit any dynamic interfering moments that adversely affect seeker control. For the above part of the work, a static balance of the first order of magnitude was assumed, i.e. reducing the distance between the centres of mass of the seeker components and the point of intersection of the axis of rotation of the outer and inner housings to the following values:

- position of the centre of mass of the rotor in relation to the axis x_r, y_r, z_r :
 $x_1 = 0 \text{ m} ; y_1 = 0.00128 \text{ m} ; z_1 = 0.000234 \text{ m}$

- position of the centre of mass of the inner housing in relation to the axis x_{cw}, y_{cw}, z_{cw} :

$$x_2 = 0 \text{ m} ; y_2 = 0.000642 \text{ m} ; z_2 = 0.001854 \text{ m}$$

- position of the centre of mass of the outer housing in relation to the axis x_{cz}, y_{cz}, z_{cz} :

$$x_3 = -0.0063 \text{ m} ; y_3 = -0.00122 \text{ m} ; z_3 = -0.00192 \text{ m}$$

The results of the computer simulations, taking into account the seeker static balance, is shown in Figs. 13-18.

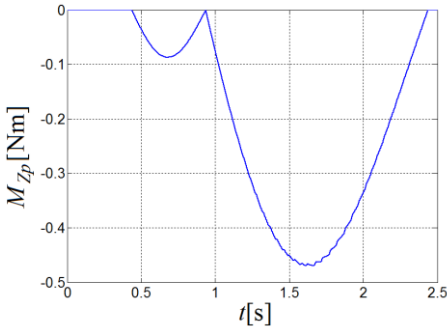


Fig. 13. Moment of force interference acting on the outer housing after the balance

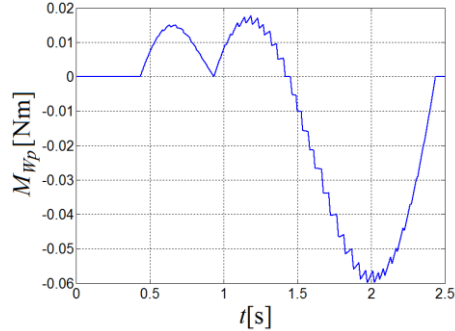


Fig. 14. Moment of force interference acting on the inner housing after the balance

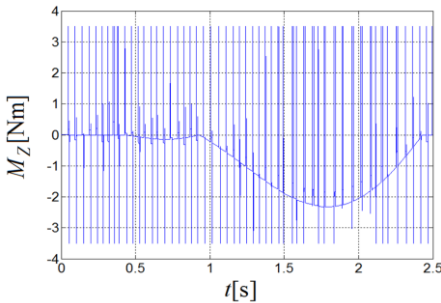


Fig. 15. Control moment of the outer housing without taking into account balance of the seeker

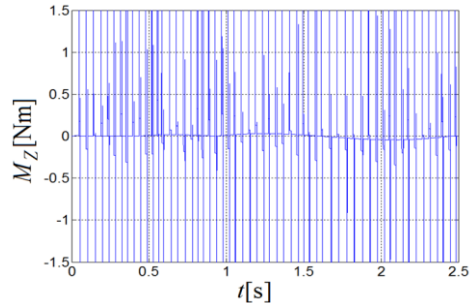


Fig. 16. Control moment of the outer housing taking into account balance of the seeker

Figures 13-14 present the resultant dynamic moments acting on the individual control housings of the seeker, taking into account the static balance. Figures 15-18 presents the moments controlling the individual housings of the seeker with and without taking into account its balance.

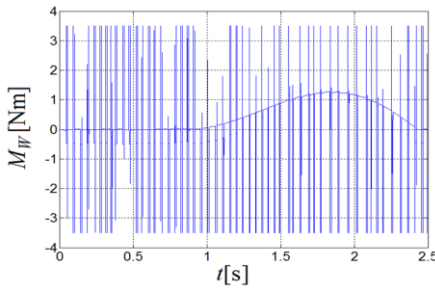


Fig. 17. Control moment of the inner housing without taking into account balance of the seeker

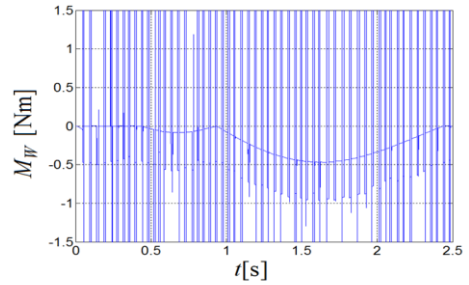


Fig. 18. Control moment of the inner housing taking into account balance of the seeker

3.4. Impact of disruptions during the launch of the missile on the stability of seeker operation

A mathematical model describing the stability of operation of the scan-track seeker was derived with the use of Lyapunov’s direct method. This model was presented in work [14], and extended in the above subsection, taking into account in the seeker axis motion equations (12, 13) interfering moments M_{Wp} and M_{Zp} . Selected results are presented below of tests on the stability of seeker operation during the launch of the missile after taking into account its static balance.

Figures 19-20 present examples of the stability of seeker operation for the maximum rotor rotational speeds, while Figs. 21-22 present examples of the stability of seeker operation for the maximum angular velocities of the outer and inner housings.

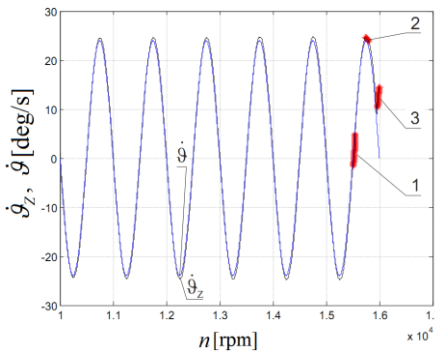


Fig. 19. Influence of rotational speed of the rotor on stability control (inner housing) during missile launch

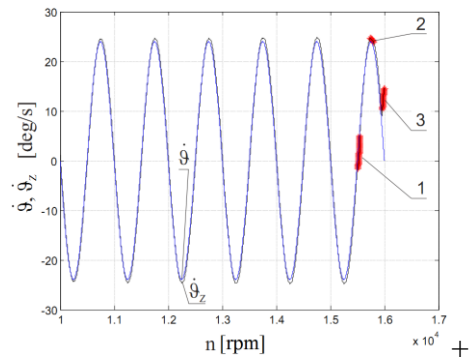


Fig. 20. Influence of rotational speed of the rotor on stability control (outer housing) during missile launch

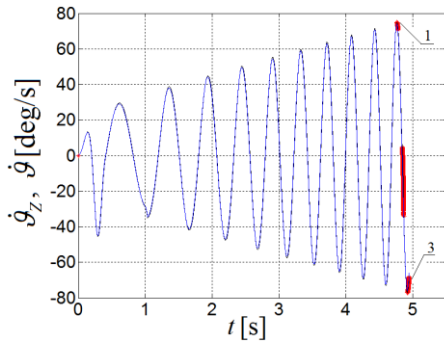


Fig. 21. The maximum angular velocity of the inner housing

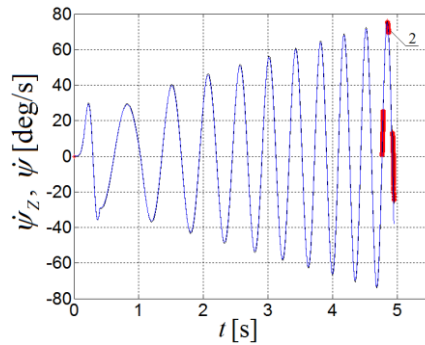


Fig. 22. The maximum angular velocity of the outer housing

The areas of instability in seeker operation numbered and marked in red in Fig. 21 correspond to the same areas in Fig. 22.

4. CONCLUSION

The analysis shows that the adverse inputs acting on the individual elements of the scanning and tracking IR seeker, in the form of dynamic moments occurring mainly in the control system, take place during launch of the missile. The most significant impact on the formation of this type of disruption result from the static imbalance of the rotor, the outer housing, and the inner housing as well as longitudinal overloads occurring during the launch of the missile.

The impact of the seeker dynamic loads triggered by the overloads occurring during the launch of the missile may be effectively reduced by balancing the seeker statically. By comparing the test results presented in section 3.2 with the results presented in section 3.3, it may be stated that there was a considerable drop in the values of interfering moments as a result of the static balance process. By comparing the values of the interfering moments before and after balancing the seeker, it may be stated that balancing gave an average drop of more than 200%, which in turn caused a favourable drop in the values of moments controlling the seeker by more than 50%. From the test results presented in section 3.4, it appears that with incorrectly set parameters for the programmed motion for the seeker axis control, the area of unstable operation can be entered with different ranges of inclinations and angular velocities of the individual housings. For the seeker parameters provided in section 3.1, it is possible to control inclinations of its individual housings for a maximum angular velocity not exceeding 70 deg/s, as illustrated in Figs. 21 and 22.

From Figs. 19 and 20, it appears that with angular velocities of the individual housings of the seeker ranging from -25 to 25/s, above a rotor rotational speed of approx. 15,000 rpm, the seeker starts to lose stability.

REFERENCES

- [1] Gapiński Daniel. 2008. *Optyczny koordynator skanujący*. Patent PL 199721 B1.
- [2] Gapiński Daniel, Zbigniew Koruba, Izabela Krzysztofik. 2014. „The model of dynamics and control of modified optical scanning seeker in anti-aircraft rocket missile”. *Mechanical System and Signal Processing* 45(2) : 433-447.
- [3] Gapiński Daniel, Izabela Krzysztofik, Zbigniew Koruba. 2014. „Analysis of the dynamics and control of the modified optical target seeker used in anti-aircraft rocket missiles”. *Journal of Theoretical and Applied Mechanics* 52(3) : 629-639.
- [4] Gapiński Daniel, Izabela Krzysztofik. 2014. „The process of tracking an air target by the designed scanning and tracking seeker”. In *Proceedings of the 15th International Carpathian. Control Conference (ICCC)*, Velke Karlovice, Czech Republic: 129-134.
- [5] Gapiński Daniel, Konrad Stefański. 2014. „Control of designed target seeker, used in self-guided anti-aircraft missiles, by employing motors with a constant torque”. *Aviation* 18: 20-27.
- [6] Adamski Mirosław Jan. 2009. Obrona samolotów i śmigłowców przed atakiem z ziemi i powietrza. W *Materiały konferencji nt. Systemy przeciwlotnicze i obrony powietrznej*, Ośrodek Badawczo-Rozwojowy Sprzętu Mechanicznego Tarnów.
- [7] Kowaleczko Grzegorz, Michał Wachłaczko. 2012. „Aircraft dynamics during flight in icing conditions”. *Journal of Theoretical and Applied Mechanics* 50(1) : 269-284.
- [8] Koruba Zbigniew. 2008. *Elementy teorii i zastosowań giroskopu sterowanego*. Monografie, Studia, Rozprawy M 7. Kielce: Wydawnictwo Politechniki Świętokrzyskiej.
- [9] Koruba Zbigniew. 2001. *Dynamika i sterowanie giroskopem na pokładzie obiektu latającego*, Monografie, Studia, Rozprawy 25. Kielce: Wydawnictwo Politechniki Świętokrzyskiej.
- [10] Milewski Stanisław, Jan W. Kobierski, Mirosław Chmieliński. 2012. „Trenażery morskich zestawów raketowo-artyleryjskich”. *Zeszyty Naukowe Akademii Marynarki Wojennej* LVII(1) : 33-53.
- [11] Żak Andrzej. 2008. „Ship’s Hydroacoustics Signatures Classification”. *Archives of Acoustics* 33(4S) : 85-90.

- [12] Gapiński Daniel, 2016. „Analysis of impact of disruptions coming from a ship on the accuracy of determining the location of the tracked air target by the modified optoelectronic scanning and tracking IR seeker”. *Zeszyty Naukowe Akademii Marynarki Wojennej* LVII(1) : 33-53.
- [13] Sztab Generalny Wojska Polskiego – Inspektorat Logistyki. 1996. *Przenośny Przeciwlotniczy Zestaw Raketowy Grom-I – opis techniczny i instrukcja eksploatacji*. Warszawa: Wydawnictwo MON.
- [14] Gapiński Daniel, Izabela Krzysztofik, Zbigniew Koruba. 2015. „Stabilność zaprojektowanego koordynatora skanującego w przeciwlotniczym pocisku raketowym”. *Problemy mechatroniki. Uzbrojenie, lotnictwo, inżynieria bezpieczeństwa – Problems of Mechatronics. Armament, Aviation, Safety Engineering* 6(1) : 56-70.

Analiza wpływu zakłóceń pochodzących od startu pocisku raketowego na stabilność pracy zaprojektowanej głowicy skanująco-śledzącej

Daniel GAPIŃSKI

*Politechnika Świętokrzyska, Wydział Mechatroniki i Budowy Maszyn,
Al. 1000-lecia Państwa Polskiego 7, 25-314 Kielce*

Streszczenie. W pracy przedstawiono wyniki badań mających na celu określenie wpływu zakłóceń pochodzących od startu pocisku raketowego na stabilność pracy zaprojektowanej, optoelektronicznej głowicy skanująco-śledzącej. Podstawowym zadaniem głowicy jest wykrycie, a następnie precyzyjne śledzenie wykrytego celu powietrznego. W badaniach uwzględnione zostały zakłócenia dynamiczne pochodzące od przeciążeń działających na głowicę w trakcie startu pocisku raketowego. Wyniki badań zaprezentowano w formie graficznej.

Słowa kluczowe: mechanika, głowica samonaprowadzająca, przeciążenia, pocisk raketowy, faza startu